

Critical parameters and spherical confinement of H atom in screened Coulomb potential

Amlan K. Roy*

Division of Chemical Sciences,

Indian Institute of Science Education and Research Kolkata,

Mohanpur Campus, Nadia, 741246, India

Abstract

Critical parameters in three screened potentials, namely, Hulthén, Yukawa and exponential cosine screened Coulomb potential are reported. Accurate estimates of these parameters are given for each of these potentials, for all states having $n \leq 10$. Comparison with literature results is made, wherever possible. Present values compare excellently with reference values; for higher n, ℓ , our results are slightly better. Some of these are presented for first time. Further, we investigate the spherical confinement of H atom embedded in a dense plasma modeled by an exponential cosine screened potential. Accurate energies along with their variation with respect to box size and screening parameter are calculated and compared with reference results in literature. Sample dipole polarizabilities are also provided in this case. The generalized pseudospectral method is used for accurate determination of eigenvalues and eigenfunctions for all calculations.

Keywords: Screened Coulomb potential, Hulthén potential, Yukawa potential, critical screening, spherical confinement, generalized pseudospectral method.

*Email: akroy@iiserkol.ac.in, akroy6k@gmail.com, Ph: +91-3473-279137, Fax: +91-33-25873020.

I. INTRODUCTION

Screened Coulomb potentials, $V(r) = -\frac{Z}{r} \sum_{k=0}^{\infty} V_k(\delta r)^k$, play a significant role in microscopic fields. They are often used as approximations to a number of interaction potentials in physics and chemistry, including atomic, molecular physics and quantum chemistry. When used in connection with atomic systems, Z refers to atomic number, while the screening parameter δ relates to different things in different branches. An enormous amount of work has been done on various aspects of these interacting potentials spanning nearly six decades.

Our current communication focuses on three screened potentials, namely Hulthén, Yukawa and exponential cosine screened Coulomb (ECSC) potential. First one is an important short-range potential with relevance in atomic, solid-state and chemical physics; it is a special case of Eckart potential. In smaller r region, both Hulthén and Yukawa potentials resemble Coulomb potential, while they decay monotonically exponentially to zero in larger r region. Other than the $\ell = 0$ states of Hulthén potential [1], *exact* analytical results remain unavailable for any of these systems; this has inspired a vast amount of publications for their bound and continuum states. Literature is quite extensive and we cite here some selected works. Bound states of Hulthén potentials are studied by variational [2, 3], shifted $1/N$ expansion [5], perturbation [6], generalized pseudospectral (GPS) [7], asymptotic iteration [8], factorization [9], Nikiforov-Uvarov [11], supersymmetry [12, 13], numerical [4] method, an algebraic approach [10], as well as numerous approximation schemes for centrifugal term [14–16], Laguerre pseudospectral method [17], etc. Likewise, bound states of Yukawa potential were also investigated by a host of approaches such as, combined Padé approximation and perturbation theory [18], variational [19], asymptotic iteration method [20], within the frame of Riccati equation [21], tridiagonal matrix approach through a suitable Laguerre basis [22], generalized parametric Nikiforov-Uvarov [23], a direct method [24] within Green-Aldrich approximation for centrifugal term, etc.

Recently, there has been a surge of interest in the ECSC potential in solid-state, nuclear, plasma physics and field theory. Some of these are: one-electron atoms in various different shielding environments [25–29], ground and excited resonances of He, H^- [30–33], molecular H_2^+ [34] in dense plasma using highly correlated wave function, two-electrons embedded in plasma within the configuration interaction framework [35], bound-state energies, polarizabilities, oscillator strengths of He [36], and etc. Since exact analytical results are not

available for this potential, an impressive amount of work has been reported for their eigen-spectra. For example, variation and perturbation method [37], and Ecker-Weizel [38, 39] and hypervirial-Padé [40] approximation, a dynamical group approach [41], hypervirial equation with Hellman-Feynman theorem [42], a numerical method [43], large-N expansion [44], shifted $1/N$ expansion [45], asymptotic iteration [46], perturbation [47], J-matrix [48], Ritz variation [49], GPS [50], Laguerre pseudospectral [17] method etc.

A distinctive feature that characterizes screened potentials is the presence of a *limited* number of bound states (in contrast to Coulomb potential). For each (n, ℓ) eigenstate, there exists a certain threshold value of screening parameter at which the binding energy of a given level in question becomes zero. That means, beyond this *critical* screening parameter ($\delta = \delta_c$), no bound states could be found, so that at this point, $E(\delta_c) = 0$. While one can find a huge amount of reference works for bound and resonant states of these potentials (as mentioned earlier), same for critical screening is rather scarce. Nevertheless, a few results are available in the literature, which are cited herein. These are published for Hulthén potential in [2, 51, 52], Yukawa potential in [19, 53, 54] and ECSC potential in [37, 39, 43, 48, 54]. Very recently, the critical parameters of $1sns\ ^{1,3}S^e$ and $1snp\ ^{1,3}P^o$ ($n \leq 5$) states of He immersed in weakly coupled Debye plasma, modeled by screened Yukawa potential, have been studied [55] as well. A primary objective of this work is to report accurate estimates of critical parameters for all three above mentioned potentials. To this end, all 55 states corresponding to $n \leq 10$ are considered systematically. For this, we employ the GPS method which has been demonstrated to produce quite reliable and accurate results for a variety of physically and chemically important systems including quantum confinement [7, 50, 56–60].

A secondary objective of this work is to investigate spherical confinement of H atom embedded in dense plasma modelled by ECSC potential. This takes inspiration from a recent publication [29], where interaction of such a system with short laser pulses in femtosecond regime was studied recording the effects of confinement radius, Debye screening length as well as laser parameters such as strength, shape, frequency and duration of pulse. Quantum confinement of H atom and other central potentials within an impenetrable spherical cavity has been a subject of much current interest. Many interesting, fascinating phenomena occur under such small spatial dimensions relative to the corresponding *free* systems. Literature on the topic is vast and rich; interested reader may consult the special issues in *Advances in Quantum Chemistry* [61] as well as the recent book [62] and numerous references therein. A

detailed analysis of the energy spectrum is presented here considering the effect of confinement radius and screening parameter on energy levels. Both low and high-lying states are treated for *small, medium and large* r_c . Additionally some specimen dipole polarizabilities are given as well. Giving a brief account of the method in Sec. II, we proceed for results in Sec. III. A few remarks are made in Conclusion in Sec. IV.

II. METHOD OF CALCULATION

The GPS method has been shown to be a simple useful and powerful approach for a variety of physical systems. They were discussed previously in a number of communications [7, 50, 56–60]; hence not repeated here. Spherical confinement of a particle in a central potential is modeled, without any loss of generality, by the following radial non-relativistic Schrödinger equation (atomic unit employed unless otherwise mentioned):

$$H\psi_{n,\ell}(r) = \left[-\frac{1}{2} \frac{d^2}{dr^2} + \frac{\ell(\ell+1)}{2r^2} + v(r) + v_c(r) \right] \psi_{n,\ell}(r), \quad (1)$$

where n, ℓ signify usual radial and angular quantum numbers, while $v(r)$ characterizes the particular screening potential under consideration. For corresponding *free* systems, $v_c(r) = 0$, whereas confinement is achieved by the following equation (r_c denotes confining radius),

$$v_c(r) = \begin{cases} +\infty & r > r_c \\ 0, & r \leq r_c. \end{cases} \quad (2)$$

Here we are interested in the following three cases,

$$v(r) = \begin{cases} -\frac{\delta e^{-\delta r}}{1-e^{-\delta r}} & \text{Hulthén potential} \\ -\frac{e^{-\delta r}}{r} & \text{Yukawa potential} \\ -\frac{e^{-\delta r}}{r} \cos(\delta r) & \text{ECSC potential.} \end{cases} \quad (3)$$

For convenience, same screening parameter δ is used for all three. Eigenvalues, eigenfunctions are obtained by solving Eq. (1) satisfying the boundary condition $\psi_{n,\ell}(0)$ finite and $\psi_{n,\ell}(r_c) = 0$.

A key feature of this method is that a given function defined in the semi-infinite domain $r \in [0, \infty]$ is approximated by an N -th order polynomial in finite interval $[-1, 1]$, such that at the *collocation points*, approximation is *exact*. This facilitates working in a *non-uniform*,

TABLE I: Estimated critical screening parameters of Hulthén, Yukawa and ECSC potential for some low-lying states having $n = 1 - 5, \ell = 0 - 4$. See text for details.

State	δ_c (Hulthén)		δ_c (Yukawa)		δ_c (ECSC)	
	PR [†]	Ref.	PR [†]	Ref.	PR [†]	Ref.
1s	2.00000000	2.000000 ^a	1.190610	1.190612 ^b , 1.190612 ^c	0.7205240	0.7115 ^d , 0.7131 ^e , 0.72052408 ^f , 0.72055425 ^g
2s	0.49999999	0.500000 ^a	0.310199	0.310209 ^c	0.1666172	0.18605 ^e , 0.1666176 ^f , 0.16656630 ^g
3s	0.22222222	0.222222 ^a	0.139466	0.139450 ^c	0.07243689	0.08828 ^e , 0.07243699 ^f , 0.07242453 ^g
4s	0.1249999	0.125000 ^a	0.078825	0.078828 ^c	0.04042716	0.0513 ^e , 0.04042722 ^f , 0.04042424 ^g
5s	0.0799999	0.080000 ^a	0.050580	0.050583 ^c	0.02578729	0.02578730 ^f , 0.02578635 ^g
2p	0.37693599	0.376936 ^a , 0.376759 ^h	0.220216806	0.220216806 ^c	0.1482050325	0.143 ^d , 0.14820503 ^f , 0.148205032 ^g
3p	0.18648588	0.186486 ^a , 0.186364 ^h	0.112710498	0.112710498 ^c	0.0687121435	0.066 ^d , 0.06871214 ^f , 0.068712143 ^g
4p	0.1104912	0.110491 ^a , 0.110410 ^h	0.067885376	0.067885376 ^c	0.0392634011	0.037 ^d , 0.03926340 ^f , 0.039263401 ^g
5p	0.0728634	0.072863 ^a , 0.072806 ^h	0.045186248	0.045186248 ^c	0.0253156252	0.024 ^d , 0.02531562 ^f , 0.0253156248 ^g
3d	0.15766196	0.157662 ^a , 0.157659 ^h	0.091345120	0.091345120 ^c	0.0635815461	0.062 ^d , 0.06358154 ^f , 0.063581546 ^g
4d	0.09756383	0.097564 ^a , 0.0975606 ^h	0.058105052	0.058105052 ^c	0.0374050483	0.036 ^d , 0.03740505 ^f , 0.037405048 ^g
5d	0.06610780	0.066108 ^a , 0.0661043 ^h	0.040024353	0.040024353 ^c	0.0245000141	0.024 ^d , 0.02450001 ^f , 0.024500014 ^g
4f	0.08640509	0.086405 ^a , 0.08640507 ^h	0.049831132	0.049831132 ^c	0.0352412421	0.035 ^d , 0.03524124 ^f , 0.035241242 ^g
5f	0.05997272	0.059973 ^a , 0.05997268 ^h	0.035389389	0.035389389 ^c	0.0234821564	0.023 ^d , 0.02348216 ^f , 0.023482156 ^g
5g	0.05450531	0.054505 ^a , 0.05450531 ^b	0.031343552		0.0223714239	0.022 ^d , 0.02237142 ^f , 0.022371423 ^g

^aRef. [2].

^bRef. [19].

^cRef. [54].

^dRef. [37].

^eRef. [39].

^fRef. [43].

^gRef. [48].

^hRef. [52].

[†]PR implies Present Result.

optimal spatial discretization, where a relatively smaller number of radial point leads to sufficiently good accuracy. Through a non-linear mapping and a symmetrization procedure, this generates a finer mesh at smaller r and cruder mesh at larger r , preserving similar kind of accuracy in both these regions. Eventually this leads to *symmetrical eigenvalue* problem, which can be easily solved accurately by means of standard routines (from NAG libraries) available. Energy calculations were performed with successive incremental changes in δ ; critical parameters were recorded by noting a change in the sign of energy values.

III. RESULTS AND DISCUSSION

A. Critical screening

At first, we discuss δ_c values for all $n \leq 5, \ell = 0 - 4$ states of Hulthén potential in columns 2, 3 of Table I. The remaining 45 states corresponding to $6 < n \leq 10$ are presented in Table S1 of the *Supporting Document*. The presented results here and in following tables were thoroughly checked for convergence by running a series of calculations changing length of grid (see discussion below) and mapping parameter (see GPS references cited earlier for its definition); which we employ as 25. It is found that the results are insensitive towards variations in number of radial points (we used 200). As mentioned earlier, some literature results are available for all the states considered, which are duly quoted for comparison. First definitive attempt was made in [51], where reasonably good estimates were reported for $1s, 2p, 3d, 4f, 5g$ and $10m$ states by means of a perturbation theory summation method, nearly three decades ago. Thus, for above mentioned states, δ_c 's of 2.0000, 0.3768, 0.1577, 0.0864, 0.0545 and 0.0133 respectively, match up to three to four places in the decimal with present as well as other available literature values. Later, these were revisited in the numerical calculation of [2]; δ_c 's were systematically determined for all $n \leq 10$ states. Present results show decent agreement with these for all the states. About a decade ago, a variational approach [52] based on a coordinate transformation on radial variable was also suggested for their calculation (for all $p - h$ states, i.e., $\ell = 1 - 5; n = (\ell + 1)$ to 10 for each ℓ). In general, one notices good matching of GPS results with these two δ_c s; probably ours are slightly better than the former two, especially for higher n, ℓ states. It is worth mentioning here that, as the screening parameters approached critical zone, considerably larger R values were necessary; this fact was mentioned before in [7]. Similar numerical instabilities have also occurred in [52] as well, in the neighborhood of δ_c . For s states, δ_c 's are readily obtained analytically as $\delta_c = 2/n^2$ from the energy expression. Note that, a simple approximate analytic expression as the following, [63],

$$\delta_c = \frac{1}{\left(\frac{n}{\sqrt{2}} + 0.1645\ell + 0.0983 \frac{\ell}{n}\right)^2}. \quad (4)$$

was also suggested for δ_c 's in terms of quantum numbers n, ℓ , which seem to be moderately good for whole range of n, ℓ . To save space and avoid clumsiness, there are omitted here;

interested reader may find them in [2].

Next, our calculated δ_c values for Yukawa potential are tabulated in columns 4,5 of Table I, for same 15 states as in Hulthén potential; while the rest 40 states are given in Table S2 of *Supporting Document*. Reference results are notably scarce in this case. Several decades ago, these were first reported [53] via numerical integration of radial Schrödinger equation for states having $\ell = 0 - 9; n = (\ell + 1)$ to 9 for each ℓ . Later, very precise ($1.19061227 \pm 0.00000004$ in a.u.) estimate of δ_c for ground state has been reported in a variational calculation [19] through linear combination of atomic orbitals scheme. Our current approach does not offer such accuracy for ground state. Nevertheless, the agreement is quite reasonable noting that all these three methods differ only in last digit. A more systematic and accurate calculation of these parameters for $n \leq 5; \ell = 0 - 3$ states were performed in the propagation matrix solution [54]. For lowest ℓ states, some disagreement is observed between the GPS result and reference. However, for $\ell \geq 1$, the two results practically coincide with each other. For $n > 5$ states, no literature values are available other than that of [53]. Our current estimates are significantly improved and we hope these could be useful for future referencing. No results are available for $n = 10$ states. As in Hulthén potential, here also, we had to enlarge radial coordinate considerably. Generally speaking, $\ell \neq 0$ states offer better accuracy than s waves.

Now we move on to δ_c in ECSC potential, in columns 6,7 of Table I. Variationally calculated δ_c 's for ECSC potential were reported [37] for ground state and those corresponding to $\ell = 1 - 7; n = (\ell + 1)$ to 8, with moderate accuracy. Also these for ns states with $n = 2 - 4$ were reported through an Ecker-Weizel method by approximating ECSC potential by a Hulthén potential [39]. Later more accurate estimates for these parameters were published for all 36 $n \leq 8$ states via numerical [43] as well as J-matrix [48] methods. For $n \leq 6$, highly accurate critical parameters have been reported [54] through a propagation-matrix solution of the eigenvalue equation by means of some simple numerical scheme. For $n > 8$, δ_c 's remain unreported as yet. Some differences in our results with those from [43] and [48] are recorded for $\ell = 0$. Otherwise, present values are in good accord with these two. Apparently those from [48] are slightly more precise than those of [43]. As in case of the previous two potentials, here also, the critical parameters for $5 < n \leq 10$ states are provided in Table S3 of *Supporting Document*.

TABLE II: Some low-lying states of confined ECSC potential, at selected r_c , for four δ values. Reference results are taken from [29]. PR implies Present Result. See text for details.

r_c	$E_{1s}(\text{PR})$	$E_{1s}(\text{Ref.})$	$E_{2p}(\text{PR})$	$E_{2p}(\text{Ref.})$	$E_{1s}(\text{PR})$	$E_{1s}(\text{Ref.})$	$E_{2p}(\text{PR})$	$E_{2p}(\text{Ref.})$
$\delta = 0.1$					$\delta = 0.2$			
0.1	469.093037729		991.107588200		469.193031240		991.207579548	
0.5	14.8479479912		36.7588456253		14.9477963784		36.8586378426	
1	2.47390897226		8.32302110803		2.57335504819		8.42223133406	
1.5	0.53684831143		3.33079617477		0.63571857088		3.42910868123	
2	-0.02527539005	-0.02528	1.67557999210	1.67558	0.07291957244	0.07292	1.77273282657	1.77273
3	-0.32446684128		0.58032931034		-0.22765602515		0.67456878317	
5	-0.39721777698	-0.39722	0.10539295060	0.10539	-0.30218038193	-0.30218	0.19252014166	0.19252
10	-0.40088390676	-0.40088	-0.02441874085		-0.30633267927	-0.30633	0.04586711993	0.04587
50	-0.40088477463	-0.40088	-0.03246880517	-0.03247	-0.30633448845	-0.30633	0.00421458654	0.00421
100	-0.40088477464		-0.03246880518		-0.30633448845		0.00101563901	
$\delta = 0.5$					$\delta = 1$			
0.1	469.492923795		991.507436380		469.992133802		992.006385267	
0.5	15.2453781208		37.1553387499		15.7287648772		37.6328672123	
1	2.86491282463		8.71032168771		3.31149548661		9.13651977224	
1.5	0.91922572831		3.70493149798		1.32242862550		4.06841930273	
2	0.34758134919	0.34758	2.03394022194	2.03394	0.70817929642	0.70818	2.33370405788	2.33370
3	0.03025176422		0.90324729702		0.31880855543		1.09173878309	
5	-0.06497226478	-0.06497	0.35727629336	0.35728	0.13351264273	0.13351	0.41381878384	0.41382
10	-0.07749780230	-0.07750	0.10554002869	0.10554	0.04125952928	0.04126	0.10213224857	0.10213
50	-0.07768368464	-0.07768	0.00404455216	0.00404	0.00191258278	0.00191	0.00403857403	0.00404
100	-0.07768368464		0.00100973663		0.00048577694		0.00100954749	

B. Spherically confined H atom in dense quantum plasma

Now Table II offers energies of H atom confined at the center of an inert impenetrable cavity embedded in an ECSC potential. Two lowest states ($1s, 2p$) corresponding to $\ell = 0, 1$ are given at four different strengths (0.1, 0.2, 0.5 and 1) of screening parameter to cover *weak, intermediate and strong* screening. Ten r_c 's have been chosen carefully in each case representing *small, medium and large* range of confinement. As mentioned in Sec. I, a substantial amount of work exists for the respective *free* system. However, to the best of our knowledge, only one reported work [29] can be found for its confinement, where some eigenvalues (within the range $r_c \leq 2 \leq 50$) were given by employing a Bernstein polynomial approach. Wherever available, present GPS energies compare quite favorably with these, offering slightly better accuracy. Many new states are given here for the first time.

Now, some representative moderately low-lying states of ECSC potential inside a spherical

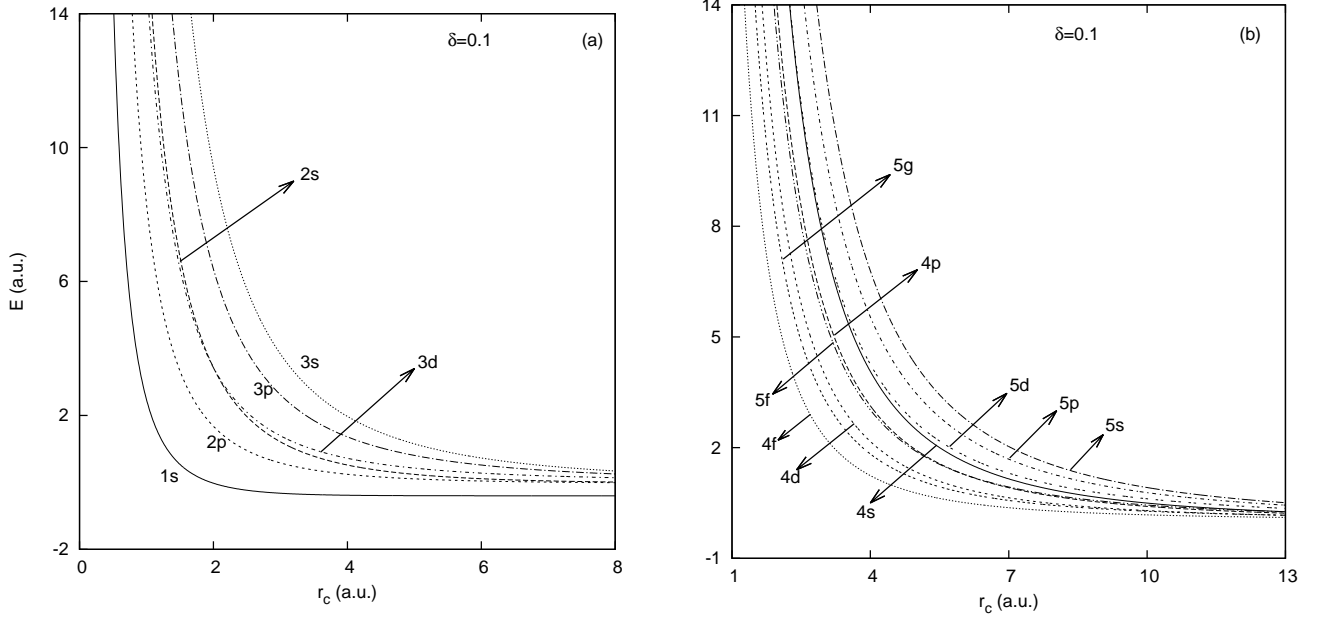


FIG. 1: Energy variations in compressed ECSC potential, with respect to r_c , for $\delta = 0.1$: (a) 6 states belonging to $n = 1, 2, 3$; (b) 9 states corresponding to $n = 4, 5$.

enclosure are offered in Table S4 of *Supporting Document*; energies are produced for all 7 states corresponding to $n = 3, 4$, for a fixed screening parameter, $\delta = 0.02$. Ten selected r_c , viz., 0.1, 0.5, 1, 2, 5, 10, 20, 30, 50 and 100 a.u., are chosen to scan the whole range of confinement. Similar to the confined H atom or Hulthén potential case [60], for a given δ_c , starting from a large positive value at smaller r_c , energy steadily decreases monotonically, crossing zero and becoming negative at certain r_c , eventually approaching a constant value at a sufficiently large r_c thereafter. Available reference energies are provided at four r_c , viz., 2, 5, 10 and 50 respectively, which seem to match rather well with present energies. To the best of our knowledge, no further attempt is known for these states, and hopefully they may constitute a useful set of reference for future works in this direction.

Above variations of isotropic compression of energies of ECSC potential in Table II are clearly depicted in energy vs. r_c plots in Fig. 1, for a fixed $\delta = 0.1$. In left panel (a), these are given for all six states corresponding to $n = 1 - 3$; (b) shows similar plots for all nine states belonging to $n = 4, 5$. Both positive, negative energies are considered in all cases. Ranges of energy and r_c axes differ from each other in these plots to clearly visualize the effects. Generally, shapes of these curves appear quite similar to each other; normally they also remain well separated (and parallel) for smaller r_c merging at a sufficiently large r_c . Very small confinement is avoided for appreciation of figures. As r_c is gradually reduced towards

lower values, energies exhibit a sharp increase. Consistent with confinement in isotropic confinement in central potentials, starting from an initial high positive value, energies tend to fall off rapidly monotonically with increase in r_c , finally approaching energy of corresponding free system smoothly and thereafter assumes a constant value. With decrease in r_c , energies change sign from negative to positive passing through a zero at critical cavity radius. One also notices crossing between some of these levels at certain r_c 's; in other words, these states become degenerate at those respective r_c 's. Some such pairs are $(2s, 3d)$ in (a); $(4s, 5d)$, $(4p, 5f)$ in (b), besides $(3p, 4f)$ (not shown), which is reminiscent of *simultaneous degeneracy* encountered in confined H atom. Furthermore, it is found that, for a specific δ , with decrease in r_c , states having same ℓ and different n maintain separation; no mixing occurs among them. Thus, for a particular ℓ and r_c , state with lowest n remains lowest in energy and vice versa, such that one finds the following energy ordering: $E_{1s} < E_{2s} < E_{3s} < E_{4s} \dots$; $E_{2p} < E_{3p} < E_{4p} \dots$; $E_{3d} < E_{4d} \dots$, etc. Likewise, for a specific δ , within a given n , individual ℓ levels remain well separated at a given r_c without crossing each other, finally attaining the energy of respective *free* system at a large r_c . With decrease in r_c , state with higher ℓ gets relatively stabilized such that the state with largest ℓ becomes lowest in energy and vice versa. So for a given n , the orderings are found as: $E_{2p} < E_{2s}$; $E_{3d} < E_{3p} < E_{3s}$; $E_{4f} < E_{4d} < E_{4p} < E_{4s}$, etc. Similar energy orderings were found in confined H atom and Hulthén potential [60]. As enclosure size is reduced, numerous complex energy splitting is observed, especially for states having high n, ℓ quantum numbers. Moreover, for a specific δ , level ordering follows the *same* pattern as H atom and Hulthén potential under similar spherical confinement; in the limit of $r_c \rightarrow 0$ this gives,

$$1s, 2p, 3d, 2s, 4f, 3p, 5g, 4d, 6h, 3s, 5f, 7i, 4p, 8k, 6g, 5d, 4s, 9l, 7h, 6f, 10m, 5p, 8i, \dots$$

This has been checked for several δ 's. However, as confining radius increases, energy ordering is characterized by frequent intermixing between levels belonging to different n values. In intermediate and large r_c region, different δ seems to provide different orderings.

We now discuss the effects of δ on energy changes in a spherically confined ECSC potential. Figure 2 illustrates this for six states corresponding to $n = 1, 2, 3$ at four selected r_c , namely, 0.5, 5, 12 and 50 respectively in panels (a)-(d). The δ values are varied from 0-1, while energy axis varies accordingly. For smaller confinement ($r_c = 0.5$) as in (a), energies change very small (practically remain unchanged) from their initial finite value, for

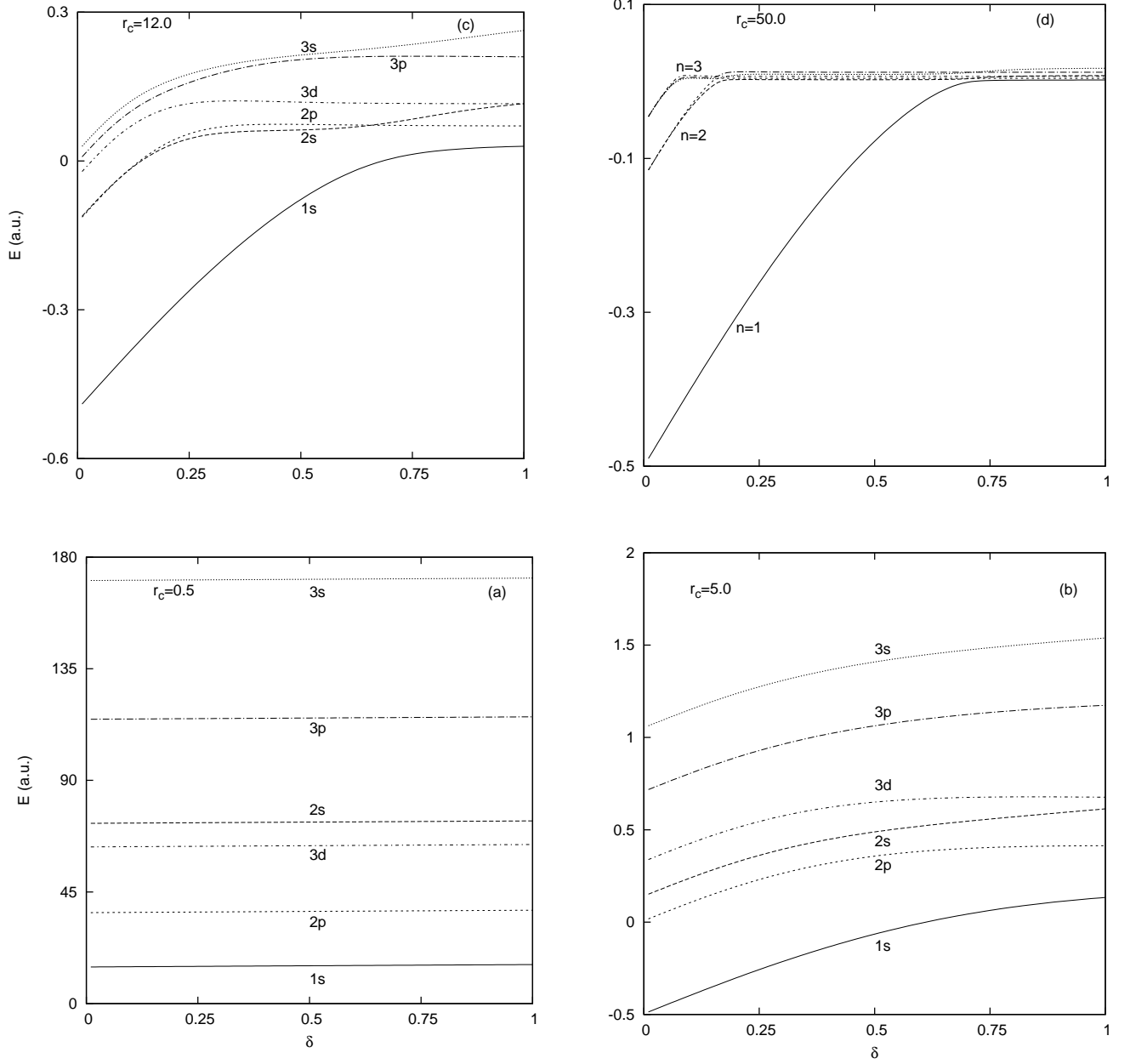


FIG. 2: Energy changes (in a.u.) in confined ECSC potential with respect to δ for 6 states having $n = 1, 2, 3$: (a)-(d) correspond to $r_c = 0.5, 5, 12$ and 50 respectively. For more details, see text.

the whole range of δ . Individual plots are parallel and maintain good distance from each other, showing no mixing/crossing amongst the levels. With slight increase in box size (such as at $r_c = 3$, which is not shown here), flat lines disappear giving rise to parallel curves. Energies drastically drop from (a) and relative separation between $2s, 3d$ levels reduces. Negative energy appears for ground state; however, energy sequence of (a) is maintained for all through out the δ range. Further increase in $r_c = 5$ in (b), bends all the curves with still

TABLE III: Dipole polarizability (in a.u.) of confined ECSC potential with respect to cage radius.

r_c	$\delta = 0.01$				$\delta = 0.1$			
	1s		2p		1s		2p	
	α_D^K	α_D^B	α_D^K	α_D^B	α_D^K	α_D^B	α_D^K	α_D^B
0.5	0.00200276	0.00203003	0.00378518	0.00420432	0.00200276	0.00203003	0.00378518	0.00420432
1	0.02847720	0.00286745	0.05871393	0.06487499	0.02847752	0.02867490	0.05871427	0.06487542
2	0.34014205	0.34015656	0.87817541	0.95985795	0.34020627	0.34022090	0.87825964	0.95995987
3	1.1732781	1.1809895	4.1219980	4.4548431	1.1743970	1.1820965	4.1240285	4.4572521
4	2.2908131	2.3578294	11.964196	12.781332	2.2971117	2.3641982	11.983098	12.803289
5	3.2040526	3.4029664	26.530803	28.013777	3.2214639	3.4215709	26.634577	28.131668
8	3.9751111	4.4528509	119.98904	122.68212	4.0188523	4.5078558	123.13619	126.02491
10	3.9986145	4.4968272	210.86134	212.42548	4.0449366	4.5567235	224.07520	225.96136
15	4.0000555	4.5000719	369.95855	370.58964	4.0466744	4.5606489	454.93699	455.94767
20	4.0000560	4.5000735	398.38484	400.95261	4.0466752	4.5606515	540.39106	548.31819
30	4.0000560	4.5000735	400.17554	403.03939	4.0466752	4.5606515	558.54036	570.79672

no mixing among them. But now $2p$ also comes closer in energy to those of $2s, 3d$ states. Further increase in $r_c = 8$ (not shown here) leads to the onset of a general shape of these plots, which continues to remain unchanged for higher r_c 's as well. Initially in the smaller screening region, any increase in δ causes considerable increase in energy until reaching a certain threshold; after this energy changes with δ tends to be less dramatic. While all the levels maintain good distance from each other through out, $2s, 2p$ remain very close to each other for the most part of δ ; only starts to branch out at $\delta \approx 0.75$. Now as r_c reaches 12 in (c), one clearly sees the three n 's making a family amongst each other. For smaller δ , energy separation between $n = 1$ and 2 are much larger compared to that between $n = 2, 3$. Once again $2s, 2p, 3d$ states continue to remain close to each other, especially for larger δ . We also notice $2s, 2p$ energies crossing at this stage. In the next r_c (15 and 20, which are not given here), the set of plots corresponding to three n continue to maintain their separate places; however evidently as δ increases more mixing amongst the states takes place and there is a tendency of all the six states to merge with increase in r_c . This is most conspicuously seen at a sufficiently large $r_c = 50$ in panel (d), where one effectively sees three plots corresponding to three n quantum numbers. Thus, state $1s$ in $n = 1$ remains a family of its own, while $2s, 2p$ forming another family practically merging at a much larger energy separation from $n = 1$, in smaller δ , and finally $3s, 3p, 3d$ coinciding with each other to form a third family. But $n = 2, 3$ families join each other at about $\delta = 0.25$, while $n = 1$ merges with them at around $\delta = 0.70$ so that after that all six states continue to assume similar energy.

TABLE IV: Comparison of [Buckingham](#) polarizabilities of ground state of *free* ECSC potential, at selected δ , with reference values of [64]. PR implies Present Result. See text for details.

Set	$\delta = 0.0$	$\delta = 0.05$	$\delta = 0.1$	$\delta = 0.15$	$\delta = 0.2$	$\delta = 0.25$	$\delta = 0.3$	$\delta = 0.4$	$\delta = 0.5$	$\delta = 0.6$
PR	4.50000	4.50839	4.56065	4.68913	4.92553	5.3139	5.9289	8.5483	17.678	90.989
Ref.	4.50000	4.50839	4.56066	4.68918	4.92576	5.3147	5.9309	8.5607	17.746	91.310

Variations similar to those in Fig. 2 were constructed for nine states belonging to $n = 4, 5$ revealing many more mixing among states. These are not produced here to save space.

At this stage, some specimen results are given for dipole polarizability of spherically confined ECSC potential in Table III. For this, we employ the simplified expressions given below, assuming that the original equations, derived for one-electron atoms in free-space, by Kirkwood and Buckingham, also hold good under confinement,

$$\alpha_D^K = \frac{4}{9}\langle r^2 \rangle^2; \quad \alpha_D^B = \frac{2}{3} \left[\frac{6\langle r^2 \rangle^3 + 3\langle r^3 \rangle^2 - 8\langle r \rangle \langle r^2 \rangle \langle r^3 \rangle}{9\langle r^2 \rangle - 8\langle r \rangle^2} \right]. \quad (5)$$

We restrict ourselves to $1s$, $2p$ states and $\delta = 0.01$ and 0.1 in panels (a), (b) respectively. Thus α_D^K and α_D^B are offered for these two states at 11 selected values of r_c covering a broad range. No results are reported for any of these. For a particular δ , both α_D^K and α_D^B gradually increase with r_c , finally reaching an asymptotic value and also satisfying the bound $\alpha_D^K \leq \alpha_D^B$. Such an inequality is known to hold for *free* spherically symmetric Coulomb potential. With increase in r_c , differences between the two α tend to increase significantly. **Multipole (dipole, quadrupole and octupole) polarizabilities for free system has been reported [64] through B -spline basis functions. Results of α_D^B for such systems at ten selected δ are compared with those. For weak to medium screening, the two results show agreement with each other. With increase in δ , the disagreements set in.** One further notices that polarizabilities for $2p$ states are higher compared to the ground state for a given δ ; moreover, the asymptotic value for $2p$ state requires much higher r_c compared to the ground state. We also observe that, increase in δ causes both α_D^K and α_D^B to increase.

Finally, Table IV offers some results on α_D^B for the ground state of *free* ECSC potential, at ten selected screening values. These are compared with the recent finite basis set calculation [64] with B -spline functions, where dipole, quadrupole and octupole polarizabilities were reported. For mild to medium screening, present results show very good agreement with these reference values. As the screening parameter increases, disagreements start to build up, which becomes significant for stronger screening.

IV. CONCLUSION

Critical parameters in three screening potentials of physical interest have been investigated systematically. Accurate values of these are reported for Hulthén, Yukawa and ECSC potentials by means of GPS method; all the 55 eigenstates on or below $n \leq 10$ are considered for all of them. Excellent agreement with best theoretical results are recorded. Some of these have not been published before. Additionally, we make an analysis of the energy spectrum in an ECSC potential when confined inside a spherically symmetric impenetrable wall, to simulate the H atom contained in a dense quantum plasma. Energy changes are followed with respect to cage radius and screening parameter. Besides, dipole polarizability and energy orderings are also discussed.

V. ACKNOWLEDGMENT

The author thanks the three anonymous referees for their constructive comments. It is a pleasure to thank Drs. Siladitya Jana and Sanjib Das for their kind help for figures. Final assistance from DST-SERB, New Delhi (Project No. EMR/2014/000838) is gratefully acknowledged.

-
- [1] S. Flügge, *Practical Quantum Mechanics* (Springer, Berlin, 1974).
 - [2] Y. P. Varshni, Phys. Rev. A **41**, 4682 (1990).
 - [3] C. Stubbins, Phys. Rev. A **48**, 220 (1993).
 - [4] M. A. Núñez, Phys. Rev. A **47**, 3620 (1993).
 - [5] A. Z. Tang and F. T. Chan, Phys. Rev. A **35**, 911 (1987).
 - [6] P. Matthys and H. De Meyer, Phys. Rev. A **38**, 1168 (1988).
 - [7] A. K. Roy, Pramana J. Phys. **65**, 1 (2005).
 - [8] O. Bayrak, and I. Boztosun, Phys. Scr. **76**, 92 (2007).
 - [9] S. H. Dong, *Factorization Method in Quantum Mechanics* (Springer, Netherlands, 2007).
 - [10] M. R. Setare and E. Karimi, Int. J. Theor. Phys. **46**, 1381 (2007).
 - [11] S. M. Ikhdair and R. Sever, J. Math. Chem. **42**, 461 (2007).
 - [12] B. Gönül, O. Özer, Y. Cançelic and M. Koçak, Phys. Lett. A **275**, 238 (2000).

- [13] S. W. Qian, B. W. Huang and Z. Y. Gu, New J. Phys. **4**, 13 (2002).
- [14] C.-S. Jia, Y.-F. Diao, L.-Z. Yi and T.Chen, Int. J. Mod. Phys. **24**, 4519 (2009).
- [15] S. M. Ikhdair, Eur. Phys. J. A **39**, 307 (2009).
- [16] S. M. Ikhdair and J. Abu-Hasna, Phys. Scr. **83**, 025002 (2011).
- [17] H. Alici and H. Taşeli, Appl. Num. Math. **87**, 87 (2015).
- [18] E. R. Vrscaj, Phys. Rev. A **33**, 1433 (1986).
- [19] O. A. Gomes, H. Chacham and J. R. Mohallem, Phys. Rev. A **50**, 228 (1994).
- [20] M. Karakoc and I. Boztosun, Int. J. Mod. Phys. E **15**, 1253 (2006).
- [21] B. Gönül, K. Köksal and E. Bakir, Phys. Scr. **73**, 279 (2006).
- [22] H. Bahlouli, M. S. Abdelmonem and I. M. Nasser, Phys. Scr. **82**, 065005 (2010).
- [23] M. Hamzavi, M. Movahedi, K.-E. Thylwe and A. A. Rajabi, Chin. Phys. Lett. **29**, 080302 (2012).
- [24] J. J. Peña, J. Morales, J. García-Martínez and J. García-Ravelo, Mol. Phys. **113**, 260 (2015).
- [25] C. Y. Lin and Y. K. Ho, Eur. Phys. J. D **57**, 21 (2010).
- [26] C. Y. Lin and Y. K. Ho, Phys. Rev. A **81**, 033405 (2010).
- [27] A. Soylu, Phys. Plasmas **19**, 072701 (2012).
- [28] T. N. Chang and T. K. Fang, Phys. Rev. A **88**, 023406 (2013).
- [29] S. Lumb, S. Lumb and V. Prasad, Phys. Rev. A **92**, 032505 (2014).
- [30] S. Kar and Y. K. Ho, Int. J. Quant. Chem. **106**, 814 (2006).
- [31] S. Kar and Y. K. Ho, Int. J. Quant. Chem. **107**, 353 (2007).
- [32] A. Ghoshal and Y. K. Ho, J. Phys. B **42**, 075002 (2009).
- [33] A. Ghoshal and Y. K. Ho, Phys. Rev. A **79**, 062514 (2009).
- [34] A. Ghoshal and Y. K. Ho, Int. J. Quant. Chem. **111**, 4288 (2011).
- [35] L. U. Ancarani and K. V. Rodriguez, Phys. Rev. A **89**, 012507 (2014).
- [36] Y.-C. Lin, C.-Y. Lin and Y. K. Ho, Int. J. Quant. Chem. **115**, 830 (2015).
- [37] C. S. Lam and Y. P. Varshni, Phys. Rev. A **6**, 1391 (1972).
- [38] R. Dutt, Phys. Lett. **73A**, 310 (1979).
- [39] P. P. Ray and A. Ray, Phys. Lett. **78A**, 443 (1980).
- [40] C. S. Lai, Phys. Rev. A **26**, 2245 (1982).
- [41] H. de Meyer, V. Fack and G. Vanden Berghe, J. Phys. A **18**, L849 (1985).
- [42] R. Sever and C. Tezcan, Phys. Rev. A **41**, 5205 (1990).

- [43] D. S. Singh and Y. P. Varshni, Phys. Rev. A **28**, 2606 (1983).
- [44] R. Sever and C. Tezcan, Phys. Rev. A **35**, 2725 (1987).
- [45] S. M. Ikhdair and R. Sever, Z. Phys. D **28**, 1 (1993).
- [46] O. Bayrak, and I. Boztosun, Int. J. Quant. Chem. **107**, 1040 (2007).
- [47] S. M. Ikhdair and R. Sever, J. Math. Chem. **41**, 343 (2007).
- [48] I. Nasser, M. S. Abdelmonem and A. Abdel-Hady, Phys. Scr. **84**, 045001 (2011).
- [49] S. Paul and Y. K. Ho, Computer Phys. Comm. **182**, 130 (2011).
- [50] A. K. Roy, Int. J. Quant. Chem. **113**, 1503 (2013).
- [51] V. S. Popov and V. M. Weinberg, Phys. Lett. A **107**, 371 (1985)
- [52] M. Demiralp, Appl. Math. Comput. **168**, 1380 (2005).
- [53] F. J. Rogers, H. C. Graboske Jr. and D. J. Harwood, Phys. Rev. A **1**, 1577 (1970).
- [54] C. G. Diaz, F. M. Fernández and E. A. Castro, J. Phys. A **24**, 2061 (1991).
- [55] Y.-C. Lin, T.-K.-Fang and Y. K. Ho, Phys. Plasmas **22**, 032113 (2015).
- [56] A. K. Roy, J. Phys. B **37**, 4369 (2004).
- [57] A. K. Roy, J. Phys. G **30**, 269 (2004).
- [58] A. K. Roy, A. F. Jalbout and E. I. Proynov, J. Math. Chem. **44**, 260 (2008).
- [59] A. K. Roy, A. F. Jalbout and E. I. Proynov, Int. J. Quant. Chem. **108**, 827 (2008).
- [60] A. K. Roy, Int. J. Quant. Chem. **115**, 937 (2015).
- [61] J. R. Sabin and E. Brändas (Eds.), *Advances in Quantum Chemistry: Theory of Confined Quantum Systems*, Parts I & II, Vols. 57 & 58, pp. 334 & 297, Academic Press, New York (2009).
- [62] K. D. Sen (Ed.), *Electronic Structure of Quantum Confined Atoms and Molecules*, pp. 253, Springer, Switzerland (2014).
- [63] S. H. Patil, J. Phys. A **17**, 575 (1984).
- [64] H. F. Lai, Y. C. Lin, C. Y. Lin and Y. K. Ho, Chin. J. Phys. **51**, 73 (2013).